Available online at http://jprm.sms.edu.pk/
Journal of Prime Research in Mathematics, 2026, 11–27

Journal of Prime Research in Mathematics

An Adaptive EWMA Dispersion Control Chart Based on Robust Estimators Under Ranked Set Sampling

Tahir Abbas[a,*], Hafiz Zafar Nazir[b], Zohaib Husssain[b], Zameer Abbas[c], Noureen Akhtar[b]

[a] *Department of Mathematics, College of Sciences, University of Sharjah 27272, Sharjah, United Arab Emirates.*

[b] *Department of Statistics, University of Sargodha, Sargodha, Pakistan.*

[c] *Government Nawaz Sharif Associate College, Sargodha, Pakistan.*

Abstract

Control charts are widely used in manufacturing and production industries to monitor and detect process variations. Traditional control charts assume that the process dispersion remains constant over time. However, in many real-world scenarios, dispersion may change over time, increasing the risk of false alarms or missed detections. To address this issue, this study improves the detection power of adaptive EWMA dispersion charts based on different robust estimators using ranked set sampling. This study constructs control limits for robust dispersion estimators using adaptive EWMA control charts. The run-length evaluation of the proposed control charts was computed using Monte Carlo simulations. The results demonstrate that dispersion-adaptive EWMA control charts based on ranked set sampling, using SD, outperform other control charts across various robust estimators. A ring-piston dataset has been used to implement the proposed study.

Keywords: Adaptive EWMA, Average run length, Industrial process, Robust estimators, RSS.
2020 Mathematics Subject Classification: 90B50, 62P25, 62P05

1. Introduction

The universe we live in is far from static; rather, it is marked by ongoing change and a profusion of unusual happenings. These differences are divided into common-cause and particular-cause variances within manufacturing and service processes. While cause variation offers a real difficulty, Common thread variation is considered a standard aspect of the operational process. Several approaches within the statistical paradigm have been developed to reduce such differences and efficiently mitigate special cause variation (e.g., [25, 11]). Statistical process control (SPC) techniques are widely used for handling variation and control charts, which come in two varieties: memory-less and memory-type, which are prominent instruments

*Corresponding author
Email addresses: TAbbas@sharjah.ac.ae (Tahir Abbas), zafar.nazir@uos.edu.pk (Hafiz Zafar Nazir), Zohaib.gujjar8316@gmail.com (Zohaib Husssain), zameerstats@gmail.com (Zameer Abbas), Noureen.akhtar@uos.edu.pk (Noureen Akhtar)

Received : 7 March 2026*; Accepted:* 20 April 2026*; Published Online:* 20 May 2026

in SPC. Memory-less control charts use only current information from the process, whereas memory-type control charts include current and prior data. Special causes of variation are a significant concern in manufacturing processes where product quality is evaluated based on unique attributes, since they can undermine the quality of the final product [4, 9, 37].

The fundamental goal of SPC is to identify and address small differences in the parameters of a manufacturing process to maintain consistent quality standards. In manufacturing businesses, detecting and controlling distinctive causes of variation is crucial, especially when product quality depends on certain traits [17]. Special sources of variation can have a major impact on product quality, making their detection and mitigation critical. This problem is being addressed using SPC techniques, such as dispersion-adaptive control charts. The manufacturing industry can improve its ability to monitor operations and maintain consistent quality standards by building dispersion-adaptive exponentially weighted moving average (AEWMA) control charts under ranked set sampling (RSS). The application of dispersion-adaptive control charts has attracted significant interest in the quality control industry. Control charts, first credited to Shewhart [36], have proven extremely useful in industrial settings, improving the quality and aesthetics of manufactured items. These Shewhart-type control charts detect substantial changes in product qualities, allowing the precise causes of variance in the manufacturing process to be identified. Subsequently, Page [29] and Roberts [34] introduced the Cumulative Sum (CUSUM) and exponentially weighted moving average(EWMA) control charts, respectively. Yashchin [38] explored control charting criteria, including graphical, computational, and statistical aspects, and discussed the properties of the Markov-type control schemes. Capizzi and Masarotto [15] proposed an AEWMA chart that uses a suitable function of the current "error" to weight historical observations in the monitored process. The AEWMA control chart demonstrated improved performance in detecting shifts in the process mean compared to traditional control charts. [22] suggested an adaptive CUSUM chart based on an EWMA-based estimator and [16] and [14] extensively studied ranked set sampling in the context of parameter estimation, showcasing its advantages over simple random sampling, i.e., the recent literature on ranked set sampling readers [3], [2], [6], [33], [31]. However, its potential application is in control charting, specifically in developing dispersion adaptive control charts. Integrating ranked set sampling with the EWMA Control chart holds promise for creating robust monitoring tools that adapt to changes in process dispersion. The development of dispersion adaptive control charts has received increasing attention due to their ability to handle changes in process dispersion. Ranked set sampling (RSS) has emerged as a sampling technique that improves the efficiency and accuracy of parameter estimation. [28] Conducted a study that evaluates the effectiveness of several phase-II CUSUM control charts for monitoring mean, median, midrange, Hodges-Lehmann, and trimean statistics, using the average run length as the performance indicator. [18] introduced a unique AEWMA chart that efficiently monitors process means by first designing an unbiased mean-shift estimator using the EWMA statistic, then adaptively updating the EWMA smoothing constant. [27] studied robust estimators based on CUSUM and AEWMA approaches under non-normality.

The proposed study investigates the robust AEWMA chart under the ranked set sampling scheme (RAEWMA-RSS; named hereafter) for monitoring the process dispersion. The dispersion estimators considered in this study included the interquartile range (IQR), standard deviation (SD), and mean absolute deviation (MAD). The adaptive EWMA chart and robust-dispersion estimators are presented in Section 2. The structure and relative analysis of the proposed RAEWMA-RSS chart are designed in Section 3. Sections 4 and 5 present the simulation results and real data examples from the manufacturing industry, respectively, and conclude with remarks in Section 6.

2. The Adaptive EWMA Chart

The design structures of the existing AEWMA chart under simple random sampling and the proposed AEWMA chart under ranked set sampling for monitoring process variability using the Huber score function are reported in this section.

2.1. Design of AEWMA

[15] proposed a powerful recursive updating mechanism of the AEWMA statistic for monitoring process observations. The plotting statistic is given by the following equation:

$$x_t = x_{t-1} + \phi(e_t), \quad y_0 = \mu_0 \tag{1}$$

As shown in the equation, μ_0 denotes the procedure average or desired result. The x_t represents the current charting statistic, x_{t-1} is the previous estimate, and $\varepsilon_t = y_t - x_{t-1}$ denotes the deviation or error between the current observation and the historical estimate. The term y_t corresponds to the incoming process observation, while $\phi(e_t)$ acts as a score function feature at time t that adaptively adjusts the update based on the magnitude of this deviation. An out-of-control signal is generated whenever the absolute deviation of the charting statistic from the target mean exceeds the control limit, i.e., when $\|x_t - \mu_0| > h$, where h is a threshold selected to achieve the desired in-control ARL.
It's worth noting that when $y_t = x_(t-1)$, Equation (1) can be modified as follows:

$$x_t = (1 - w(e))x_{t-1} + w(e)y_t \tag{2}$$

As $w(e) = \frac{\phi(e)}{e}$, and $\phi(e)$ are the scoring functions described in Equations (3), (4), and (5). This transformation reveals that the AEWMA structure is analogous to a classical EWMA, but with a data-dependent adaptive weight replacing the fixed smoothing parameter [31]. Equation (2) is comparable to the standard EWMA statistic but has a load element $w(e)$ replacing the constant λ. The $w(e)$ behaves similarly to a conventional smoothing constant, ensuring gradual updates. Equations (3) and (4), which further develop Tukey's square and Huber functions, respectively, [15] offer the following scoring functions:

$$\phi_{hu}(e) = \begin{cases} e + (1-\lambda)k, & \text{if } e < -k, \\ \lambda e, & \text{if } |e| \le k, \\ e - (1-\lambda)k, & \text{if } e > k. \end{cases} \tag{3}$$

$$\phi_{bs}(e) = \begin{cases} e\left[1 - (1-\lambda)\left(1 - (e/k)^2\right)^2\right], & \text{if } |e| \le k, \\ e, & \text{if } |e| > k. \end{cases} \tag{4}$$

Additionally, they proposed another score function, $\phi_{cb}(e)$ described in Equation (5):

$$\phi_{cb}(e) = \begin{cases} e, & \text{if } e \le -p_1, \\ -\phi_{cb}(-e), & \text{if } -p_1 < e < -p_0, \\ \lambda e, & \text{if } |e| \le p_0, \\ \phi_{cb}(e), & \text{if } p_0 < e < p_1, \\ e, & \text{if } e \ge p_1. \end{cases} \tag{5}$$

Here, $0 < \lambda \le 1$, $0 \le p_0 < p_1$, and $k \ge 0$ are parameters that must be appropriately selected. When the agreement between y_t and x_{t-1} is very low, the scoring function in Equation (3) may cause the scheme to partially disregard earlier process observations, whereas the schemes based on Equations (4) and (5) completely disregard historical data. Equation (6) shows $\phi_{cb}(.)$ is a cubic polynomial that makes $\phi_{cb}(.)$ with a continuous first derivative [10], [13], [32]:

$$\phi_{cb}(e) = \lambda e + (1-\lambda)\left(\frac{e-p_0}{p_1-p_0}\right)^2\left[2p_1 + p_0 - (p_1+p_0)\left(\frac{e-p_0}{p_1-p_0}\right)\right] \tag{6}$$

Here, λ is the smoothing parameter controlling memory, h is the control limit coefficient, while k, p_0, and p_1 are the robustness tuning constants in the score functions. This makes $\phi_{cb}(e)$ very flexible, enabling its operation over a range of e values and allowing it to approximate the score functions in Equations (3) and (4) by selecting different values for p_0 and p_1.

2.2. Dispersion Point Estimators

The selection of parameter estimator(s) is a critical problem in parameter estimation. The selection of estimator(s) is crucial in creating an efficient and robust control chart design. Process samples are often taken as reasonable subgroups of size n. When the process is stable (the process parameters do not vary over time), using an estimate based on the set of observations created by merging the subgroups into a single group is the most effective technique to estimate the process dispersion. Let θ represent the process dispersion, and $\hat{\theta}$ is the estimator of the RSS-based dispersion method. The scattering of the estimators $\hat{\theta}$ (Range, S.D., IQR, and MAD) is given below:

2.2.1. Range

The range is a very common and simple estimator of dispersion. The range (R) of a data set is the difference between its largest and smallest values. Let $w_1, w_2, \ldots, w_n$ be a random sample and $w_{(1)}, w_{(2)}, \ldots, w_{(n)}$ be an order statistic, where $W_{(i)} < W_{(j)}$, then the mathematical form of the range follows as

$$R = w_n - w_1 \tag{7}$$

Where w_n is the maximum, and w_1 is the minimum value in the data set. The range is a non-robust estimator because it is highly affected by outliers.

2.2.2. Sample Standard Deviation

The standard deviation (SD) is the most widely used estimator of dispersion, but it is not robust. The SD may be obtained by summing the squared deviations from the arithmetic mean and dividing by the total number of observations. SD is defined as

$$SD = \left(\frac{1}{n-1} \sum_{i=1}^{n} (w_i - \bar{w})^2 \right)^{1/2} \tag{8}$$

Where $\bar{w}$ denotes the corresponding mean of the sample, and w_i denotes the i^{th} observation in a sample of size n. Standard deviation is the average difference of the observations from the mean value. The sample SD is the most efficient estimator, yet research has shown that outliers significantly affect it.

2.2.3. Inter Quartile Range

The first robust estimator that will be discussed in further study is the interquartile range (IQR), which is defined as

$$\text{IQR} = \frac{Q_3 - Q_1}{1.34898} \tag{9}$$

Where Q_3 and Q_1 are the 3rd and 1st quartiles, respectively, are calculated from the sample values. The factor 1.34898 is the normalization constant that makes the IQR a consistent estimator of the standard deviation under normality since $Q_3 - Q_1 = 1.34898\sigma$ for a normal distribution. The IQR is more robust against departures from normality and outliers than the sample standard deviation.

2.2.4. Absolute median of deviations from the median

[24] proposed a new, reliable estimator based on the median of absolute deviations from the median, named as "MAD" and described as

$$\text{MAD} = 1.4826 \,\text{median}\, |w_i - \tilde{w}| \tag{10}$$

Where $\tilde{w}$ is the median of the sample. The constant 1.4826 is the consistency factor under normality. This estimator has a relatively poor efficiency under normality but is quite robust against outliers. The standard deviation (SD) is considered the most efficient estimator under normality, but is highly sensitive to outliers. The IQR will be characterized as a robust estimator with moderate efficiency and strong resistance to extreme observations. The MAD will be highlighted as a highly robust estimator with a high breakdown point (50%), though less efficient under normal conditions. The choice among these estimators is a trade-off between efficiency and robustness.

3. Proposed RAEWMA-RSS chart

The RSS scheme and the proposed RAEWMA-RSS charts have been reported in this section.

3.1. Ranked Set Sampling

Ranked set sampling (RSS) is a unique sampling technique that improves parameter estimation accuracy while reducing sample sizes compared to traditional random sampling methods. The RSS has gained popularity across various research fields for its ability to leverage ranking information to achieve more precise estimates with limited resources. Sets for sampling are selected using random sampling methods, such as simple random or systematic sampling. Once a set is chosen, all observations within it are included in the sample, retaining their original rankings. This unique characteristic of RSS enables more efficient estimation, as information from both the values and their rankings is used. The mean and variance of a population parameter estimated using RSS can be derived based on the ranking information within the sets. The RSS mean estimator is defined as the average of the ranked observations within the selected sets. Given a sample size of n sets, each containing m observations, the estimated mean (μ_{rss}) can be calculated as:
Let $X_{11}, X_{12}, X_{13}, \ldots, X_{1n}, X_{21}, X_{22}, \ldots, X_{n1}, X_{n2}, \ldots, X_{nn}$ be n independent simple random samples of each size n. Apply the RSS procedure to these n samples to obtain a ranked set sample of size n denoted by $X_{1(1:n)}, X_{2(2:n)}, X_{3(3:n)}, X_{n(n:n}$. The mean of this ranked set sample is$\bar{X}_{RSS} = \frac{1}{n}\sum_{j=1}^{n} X_{i(j:n)}$. Under perfect ranking, then, the unbiased estimator for the population means, proposed by [19], is defined as:

$$\bar{X}_{RSS} = \frac{1}{n}\sum_{i=1}^{n} X_{(i)} \tag{11}$$

with variance given by:

$$\bar{X}_{RSS} = \frac{1}{n^2}\sum_{i=1}^{n} \sigma^2_{(i:n)} \tag{12}$$

The implementation of the ranked set sampling (RSS) scheme in this study is based on several standard assumptions. It is assumed that a reliable ranking mechanism is available, either through an auxiliary variable correlated with the quality characteristic or through informed judgment, and that the ranking of units within each set is reasonably accurate. In addition, observations across sampling cycles are assumed independent, and the underlying process distribution is assumed stable within each RSS cycle. In practical manufacturing environments, these assumptions may be only approximately satisfied. Ranking errors, lack of a suitable ranking variable, or the presence of autocorrelation and process shifts may affect the efficiency of RSS and, consequently, the performance of the proposed control chart. However, the use of robust dispersion estimators (e.g., IQR and MAD) within the adaptive EWMA framework helps mitigate the impact of such imperfections.

3.2. Proposed RAEWMA-RSS charts

A novel RAEWMA-RSS chart is proposed in this section for effectively tracking dispersion shifts within a certain range. The suggested RAEWMA-RSS chart's run-length profiles are generated and examined using extensive Monte Carlo simulations. The typical RAEWMA-RSS approach assumes that the underlying process is normally distributed. The plotting statistic of the newly suggested AEWMA under the RSS method is as follows.

$$x_t = (1 - w(e_t))x_{t-1} + w(e_t)\hat{\theta}_t \tag{13}$$

Where $e_t = \hat{\theta}_t - x_{t-1}$ and $\hat{\theta}_t$ might be any choice of dispersion estimators under ranked set sampling. This control chart shows that when $x_t > UCL_t$ or $x_t < LCL_t$. There are representations of the upper control limit (UCL) and the lower control limit (LCL). The UCL and LCL of the anticipated control charts are supplied:

$$\mathrm{UCL}_t = \hat{\mu}_\theta + L\,\hat{\sigma}_\theta\sqrt{\frac{\lambda}{2-\lambda}\left(1-(1-\lambda)^{2t}\right)} \tag{14}$$

$$\mathrm{LCL}_t = \hat{\mu}_\theta - L\,\hat{\sigma}_\theta \sqrt{\frac{\lambda}{2-\lambda}\left(1-(1-\lambda)^{2t}\right)} \tag{15}$$

Where $L > 0$ is the control limit coefficient used to obtain the pre-specified in-control average run length (ARL). Table 1 presents the in-control process, $\hat{\mu}_\theta$ and $\hat{\sigma}_\theta$, and shows the expected values and standard deviations of the estimators.

Table 1: Expected values and Standard Deviations of Dispersion Estimators

	Mean				SD			
n	Range	IQR	SD	MAD	Range	IQR	SD	MAD
5	2.5717	0.7871	1.0317	0.9124	0.8127	0.3935	0.3082	0.4762
6	2.7809	0.8406	1.0323	0.9173	0.7788	0.3178	0.2646	0.3640
8	3.0889	0.8825	1.0312	0.9537	0.7377	0.2681	0.2095	0.3099
9	3.2121	0.8821	1.0289	0.9739	0.7216	0.2805	0.1905	0.3185
10	3.3172	0.8997	1.0274	0.9720	0.7085	0.2396	0.1749	0.2686

4. Performance Evaluation

To evaluate the performance of the proposed RAEWMA-RSS control chart, an extensive Monte Carlo simulation study was conducted. The simulations were performed with 1×10^5 iterations to ensure stable, reliable estimates of run-length characteristics. The designed control charts are evaluated using the average run length (ARL), a widely used performance metric for monitoring the behavior of control charts (CCs) in response to a discrete shift at a specific point [5], [23], [21]. ARL values help assess the mean of the Run Length (RL) distribution at the shift point. The ARL is defined as the average number of samples needed for a process to produce its first out-of-control signal. ARL_0 refers to the ARL when the process is in control, whereas ARL1 represents the ARL when the process is out of control (cf. [30], [35], **(author?)** [7],[8], [1], [20]). The smoothing parameters were selected as $\lambda = 0.10$, 0.15, and 0.25, corresponding to low, moderate, and relatively high memory levels in the AEWMA-RSS structure. The current study investigates subgroup sizes of n = 5 and n = 10 to examine the effect of sample size on detection performance. The control limits were calibrated to achieve a target ARL_0 of 370, in accordance with standard SPC practice (cf. [12]). The out-of-control performance was evaluated for shift magnitudes in the range $1.02 \leq \delta \leq 2$, while the robustness tuning constant was selected as $k = 1.25$, 1.5, and 2. Table 2 presents the calibrated values of the control limit coefficient h required to achieve the target in-control performance ARL_0 of 370 for different combinations of subgroup sizes n, smoothing parameters λ, and dispersion estimators (Range, IQR, SD, MAD). As λ increases (e.g., from 0.10 to 0.25), the corresponding h values generally decrease across all estimators. This occurs because a larger λ assigns more weight to current observations, increasing chart sensitivity; hence, a smaller control limit is sufficient to maintain the same ARL_0. Increasing the subgroup size from $n = 5$ to $n = 10$ results in slightly lower or stabilized h-values, reflecting improved estimation precision. Larger samples reduce variability in dispersion estimates, requiring less conservative control limits. The Range-based estimator requires substantially larger h values compared to IQR, SD, and MAD. This reflects its higher variability and sensitivity to extreme values. In contrast, IQR and SD exhibit smaller and more stable h values, indicating more reliable dispersion estimation under normal conditions.
Table 3 reports the run-length performance of the proposed AEWMA-RSS charts under normal conditions, including both in-control (ARL_0) and out-of-control (ARL_1) behavior for various shift magnitudes δ. As shown in Table 3, all proposed charts maintain the desired in-control performance, with ARL_0 values close to 370 across different n and λ values. For small shifts ($\delta = 1.02$), the IQR-based chart demonstrates superior sensitivity, with substantially lower ARL_1 (e.g., 212.9 compared to 285.13 for Range and 252.03 for SD) when λ is small ($\lambda = 0.10$). The performance of the SD-based chart is better than that of other charts for larger values of λ ($\lambda = 0.15$ and 0.25), i.e., when $\lambda = 0.25$, $n = 10$, and $\delta = 1.02$, the ARL_1

Table 2: Design Parameter (h) values for AEWMA chart for $ARL_0 \approx 370$

		$n=5$				$n=6$				$n=8$				$n=9$			
k	λ	Range	IQR	SD	MAD	Range	IQR	SD	MAD	Range	IQR	SD	MAD	Range	IQR	SD	MAD
1.25	0.10	9.9851	3.8066	2.72	3.3899	9.9999	3.4096	2.74	2.8499	10.1147	3.2139	2.75	2.7599	10.1147	3.1699	2.754	2.7299
	0.15	7.7999	3.0999	2.8045	3.1479	7.8599	2.9999	2.83	2.8469	7.8366	2.9389	2.834	2.8189	7.7999	2.9359	2.823	2.8077
	0.25	5.5899	2.9601	2.909	3.0299	5.6299	2.9132	2.928	2.9099	5.6097	2.9185	2.927	2.9099	5.6097	2.9185	2.927	2.9069
	0.50	3.3351	3.0699	3.025	3.136	3.3789	2.9599	3.039	3.0359	3.4499	2.9799	3.049	2.9979	3.5069	2.9605	3.056	2.9789
	0.75	3.2111	3.1399	3.0699	3.2399	3.2599	3.0029	3.099	3.1249	3.2794	3.0285	3.112	3.0392	3.2977	2.9795	3.114	3.0199
	0.95	3.2526	3.1699	3.097	3.2799	3.2899	3.0299	3.121	3.1399	3.3239	3.0399	3.136	3.0499	3.3380	2.9935	3.1382	3.0369
1.50	0.10	9.4111	3.6086	2.72	2.895	9.5999	3.3879	2.743	2.8099	9.5999	3.2129	2.75	2.7499	9.5599	3.1789	2.754	2.7259
	0.15	7.2699	3.0647	2.8045	2.8789	7.3299	2.9871	2.821	2.8399	7.4010	2.9389	2.834	2.8189	7.3899	2.9359	2.825	2.8077
	0.25	5.2099	2.9600	2.909	2.95	5.2599	2.9132	2.921	2.9099	5.2769	2.9185	2.927	2.9069	5.2870	2.9085	2.927	2.9069
	0.50	3.2214	3.0799	3.023	3.136	3.2710	2.9599	3.049	3.0359	3.3697	2.9849	3.049	2.9979	3.4219	2.9605	3.053	2.9789
	0.75	3.2171	3.1399	3.0799	3.2399	3.2599	3.0089	3.101	3.1249	3.2794	3.0265	3.112	3.0392	3.2977	2.9795	3.123	3.0199
	0.95	3.2526	3.1679	3.097	3.2799	3.2999	3.0298	3.121	3.1499	3.3240	3.0399	3.133	3.0499	3.3380	2.9932	3.1382	3.0279
2.00	0.10	8.4165	3.5779	2.72	2.7695	8.6299	3.3901	2.74	2.8099	8.6260	3.2129	2.75	2.7599	8.6860	3.1785	2.754	2.7299
	0.15	6.4877	3.0557	2.8055	2.8199	6.6269	2.9871	2.826	2.8299	6.6399	2.9399	2.825	2.8289	6.6746	2.9359	2.823	2.8099
	0.25	4.5999	2.9520	2.909	2.93	4.7699	2.9132	2.929	2.9099	4.7572	2.9185	2.927	2.9069	4.7582	2.9087	2.928	2.9009
	0.50	3.1599	3.0699	3.025	3.136	3.2399	2.9599	3.045	3.0349	3.3471	2.9849	3.047	2.9979	3.3999	2.9605	3.056	2.9789
	0.75	3.2161	3.1399	3.0799	3.2399	3.2599	3.0089	3.101	3.1249	3.2811	3.0265	3.109	3.0372	3.2977	2.9795	3.116	3.0199
	0.95	3.2526	3.1759	3.099	3.2799	3.2999	3.0378	3.121	3.1499	3.3260	3.0399	3.133	3.0479	3.3380	2.9832	3.1384	3.0369

Table 3: ARL values for AEWMA chart under Normal distribution with k=1.25 and $ARL_0 \approx 370$

λ	Subsample Size	Estimators	h	δ								
				1.00	1.02	1.05	1.10	1.15	1.20	1.25	1.50	2.00
0.10	$n=5$	Range	9.9851	371.2	285.13	190.37	112.8	67.72	40.04	27.15	5.58	1
		IQR	3.8066	370.2	212.90	104.92	37.19	15.46	7.86	4.38	1.5	1
		SD	2.72	369.5	252.03	121.02	46.16	24.15	15.72	11.36	4.24	1
		MAD	3.3899	370.1	274.16	181.34	93.85	53.67	32.95	22.58	6.66	1
	$n=10$	Range	10.114	368.9	275.89	188.19	101.1	59.15	35.33	22.12	3.62	1
		IQR	3.1625	369.5	171.91	49.04	10.2	4.28	2.37	1.71	1.1	1
		SD	2.754	369.5	186.08	59.95	20.67	11.46	7.59	5.64	2.37	1
		MAD	2.7399	372.4	238.11	100.77	33.06	16.36	9.75	6.47	2.32	1
0.15	$n=5$	Range	7.7999	369.3	264.14	205.35	115.6	71.28	43.57	30.18	6.1	1
		IQR	3.0999	369.2	262.02	129.11	51.77	25.54	14.64	9.49	2.71	1
		SD	2.8045	372.0	254.96	125.79	49.85	25.24	15.93	11.28	4.11	1
		MAD	3.1479	368.6	277.69	176.02	91.79	53.48	33.73	23.04	7.06	1
	$n=10$	Range	7.8362	368.7	270.30	195.53	103.1	61.24	37.42	23.94	4.01	1
		IQR	2.9299	371.3	223.02	86.70	24.32	10.22	5.64	3.67	1.45	1
		SD	2.823	368.7	192.23	67.41	21.54	11.14	7.25	5.25	2.12	1
		MAD	2.8099	371.7	239.13	113.17	40.03	19.08	11.48	7.84	2.67	1
0.25	$n=5$	Range	5.5899	370.1	287.12	200.55	111.9	71.73	43.93	29.55	6.97	1
		IQR	2.9601	371.0	255.68	153.69	74.94	41.56	25.07	17.21	4.95	1
		SD	2.909	370.2	251.38	135.65	54.28	28.18	17.04	11.67	3.96	1
		MAD	3.0299	371.9	270.02	173.33	91.63	53.97	34.55	24.21	7.79	1
	$n=10$	Range	5.6098	372.7	276.00	186.41	103.1	57.33	34.31	21.43	4.06	1
		IQR	2.9087	369.5	246.57	119.13	40.53	18.27	10.14	6.63	2.12	1
		SD	2.932	370.6	206.55	79.55	24.99	12.03	7.27	5.15	1.99	1
		MAD	2.9099	369.4	254.86	129.32	48.5	23.49	13.59	9.21	3.01	1

values for Range, IQR, MAD, and SD are 276.00, 246.57, 254.86, and 206.55, respectively. As the shift magnitude increases, all charts exhibit the expected decrease in ARL_1, confirming their ability to detect larger process changes more rapidly. Furthermore, increasing the smoothing parameter λ generally yields higher ARL_1 values, indicating reduced sensitivity but improved stability, consistent with the theoretical behavior of EWMA-type charts.

This highlights the classical trade-off: smaller λ improves early detection, while larger λ enhances stability. As the shift magnitude increases (e.g., $\delta = 1.10, 1.25$), all charts exhibit a monotonic decrease in ARL_1, which is a desirable property. The IQR and SD estimators continue to outperform MAD and Range in most cases. Larger sample sizes (e.g., $n = 10$) yield lower ARL_1 values than smaller ones (e.g., $n = 5$), particularly for small and moderate shifts. This confirms that increased sample information improves detection capability. The results suggest that the SD-based AEWMA-RSS chart performs best overall, especially for detecting small-to-moderate dispersion shifts at larger values of the smoothing parameter, followed by the IQR-based AEWMA-RSS chart. The MAD estimator offers robustness but at the cost of slower detection, while the Range-based estimator performs the worst.

Overall, Tables 2 and 3 demonstrate that proper calibration ensures comparable in-control performance, while the choice of dispersion estimator and smoothing parameter critically affects detection efficiency. The SD-based adaptive EWMA chart under ranked set sampling emerges as the most effective approach, particularly for small process shifts.

Graphical display of RAEWMA-RSS chart: Figures 1–8 illustrate the performance of the proposed RAEWMA-RSS control charts by plotting the log of out-of-control average run length ARL_1 on the vertical y-axis against the shift magnitude δ on the horizontal x-axis for different estimators, subgroup sizes n, and design parameters. The y-axis represents the expected number of samples required to signal an out-of-control condition, while the x-axis reflects the magnitude of change in process dispersion. From these plots, it is evident that ARL_1 decreases as δ increases, which is a desirable property since larger shifts should be detected more quickly. For small shifts (e.g., $\delta = 1.02$), the curves start at relatively high ARL_1 values, indicating slower detection; however, the SD-based charts show lower ARL_1 values than those of other estimators, demonstrating superior sensitivity. As the shift increases (e.g., $\delta = 1.10$ to 1.25), all curves decline, but the IQR and SD estimators decline more steeply, indicating faster detection than MAD and Range. The Range-based charts consistently remain higher on the y-axis, reflecting poorer detection efficiency. Additionally, variations across figures show that smaller values of the smoothing parameter λ shift the curves downward (lower ARL_1), enhancing responsiveness, whereas larger λ values produce smoother but slower detection. Increasing the subgroup size (n) also shifts the curves downward, indicating improved performance due to more stable estimation. Overall, these plots provide a clear visual confirmation of how estimator choice and design parameters influence the speed of detecting shifts in process dispersion.

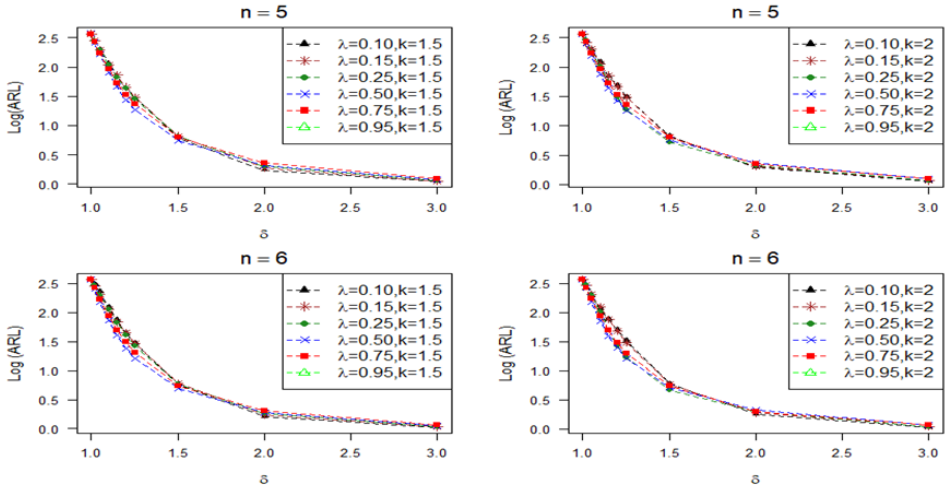

Figure 1: ARL_1 of the Proposed RAEWMA-RSS chart for the Range when $n = 5, 6$, and $k = 1.5, 2$.

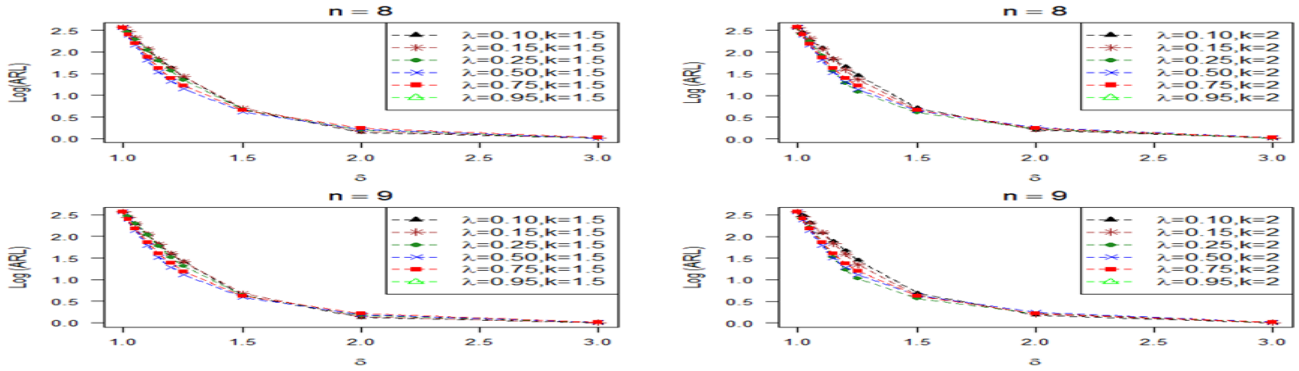

Figure 2: ARL_1 of the Proposed RAEWMA-RSS chart for the Range when $n = 8, 9$, and $k = 1.5, 2$.

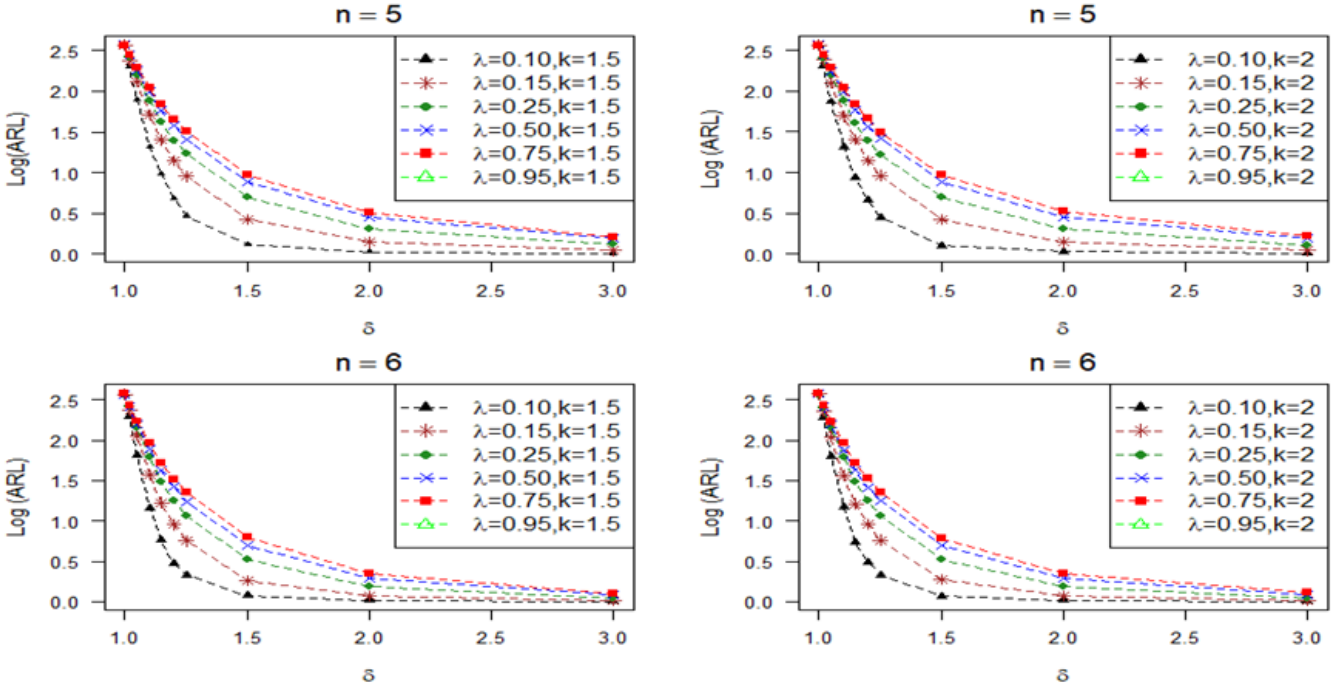

Figure 3: ARL_1 of the Proposed RAEWMA-RSS chart for the IQR when $n = 5, 6$, and $k = 1.5, 2$.

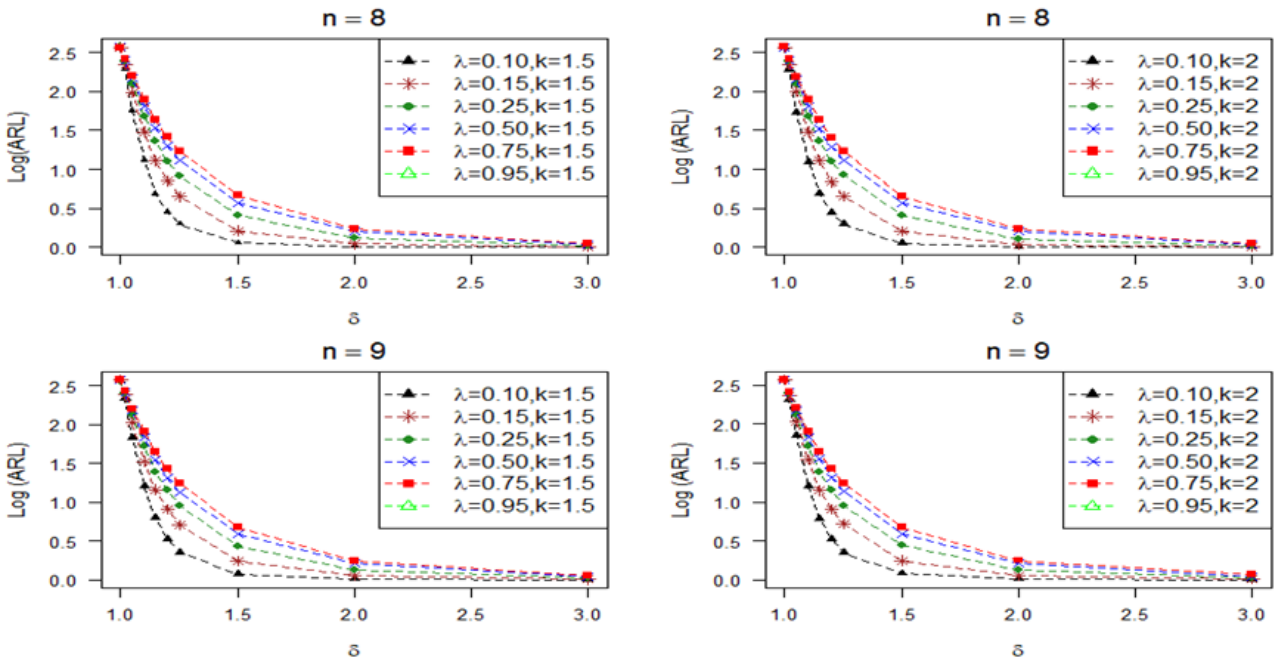

Figure 4: ARL_1 of the Proposed RAEWMA-RSS chart for the IQR when $n = 8, 9$, and $k = 1.5, 2$.

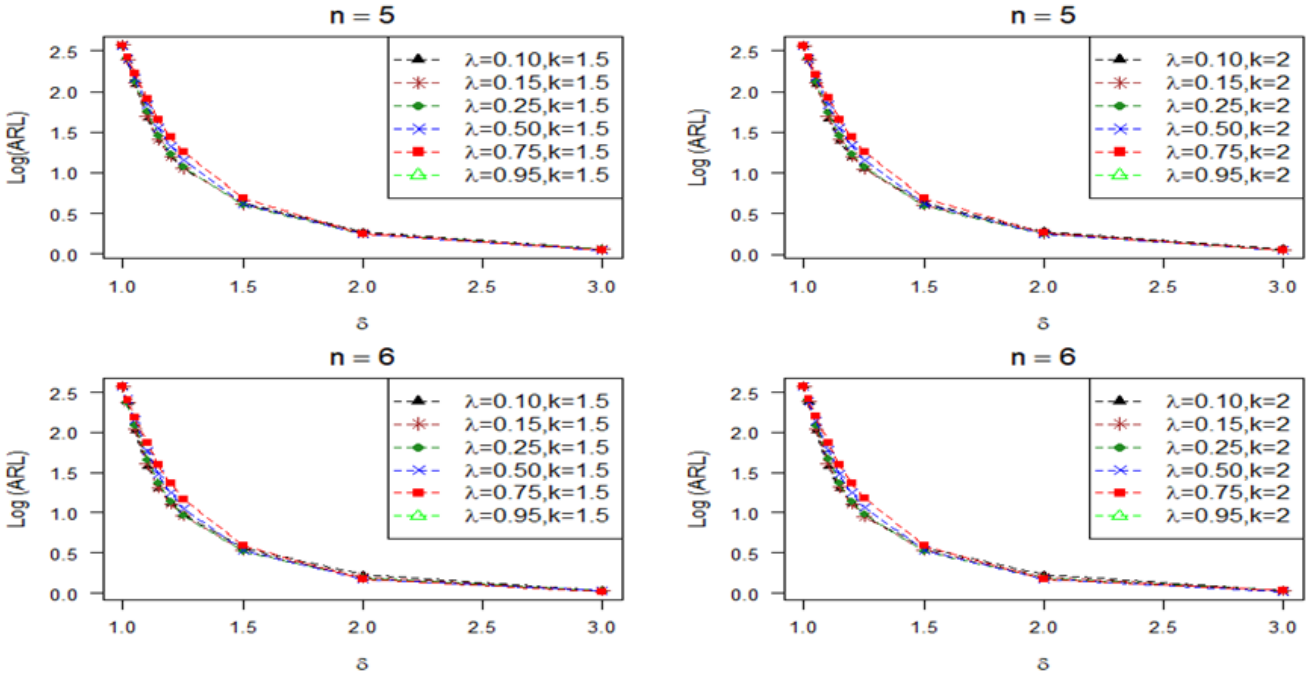

Figure 5: ARL_1 of the Proposed RAEWMA-RSS chart for the SD when $n = 5, 6$, and $k = 1.5, 2$.

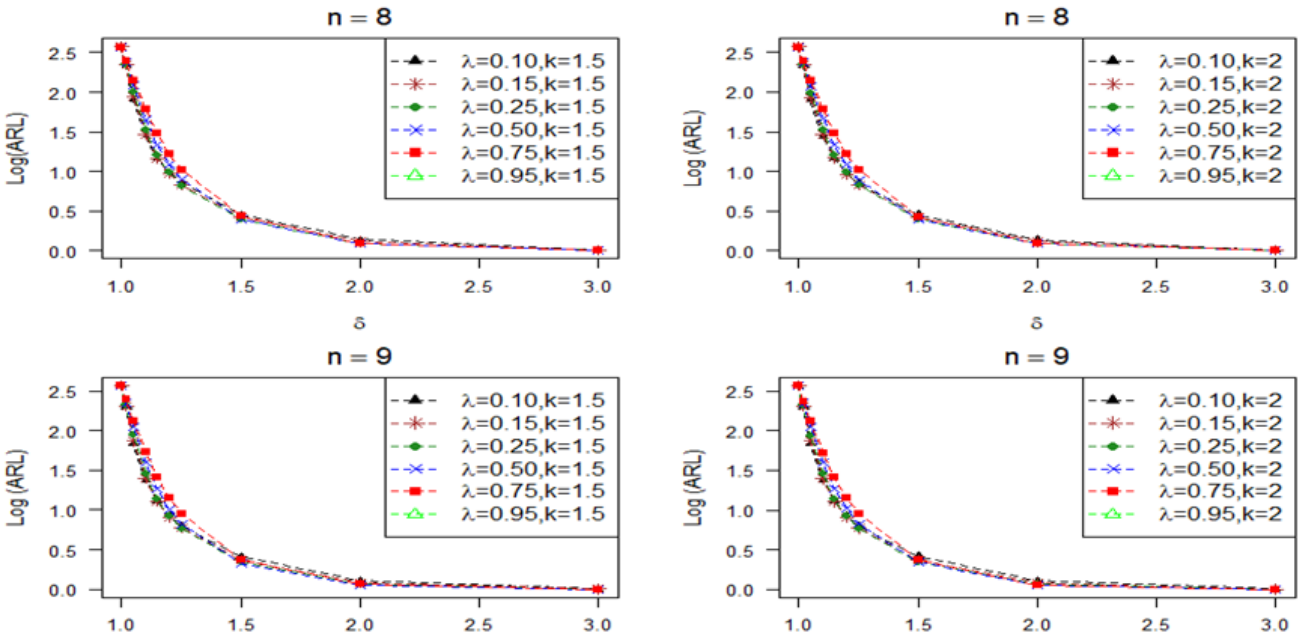

Figure 6: ARL_1 of the Proposed RAEWMA-RSS chart for the SD when $n = 8, 9$, and $k = 1.5, 2$.

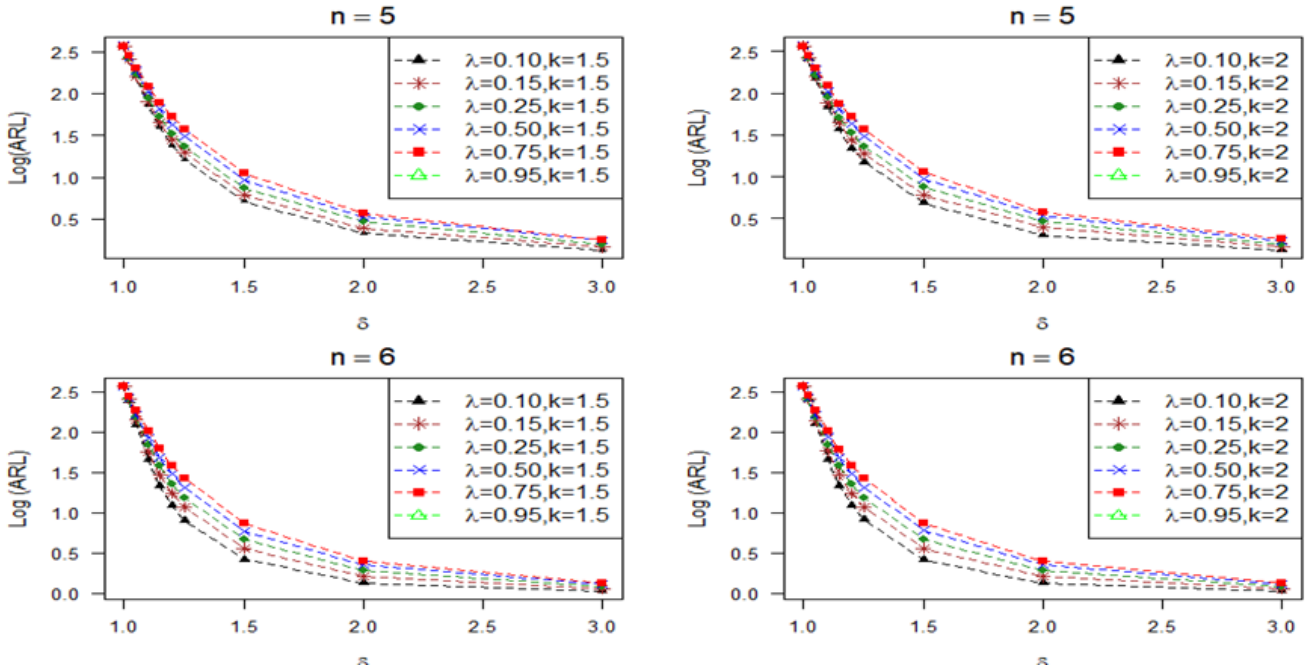

Figure 7: ARL_1 of the Proposed RAEWMA-RSS chart for the MAD when $n = 5, 6$, and $k = 1.5, 2$.

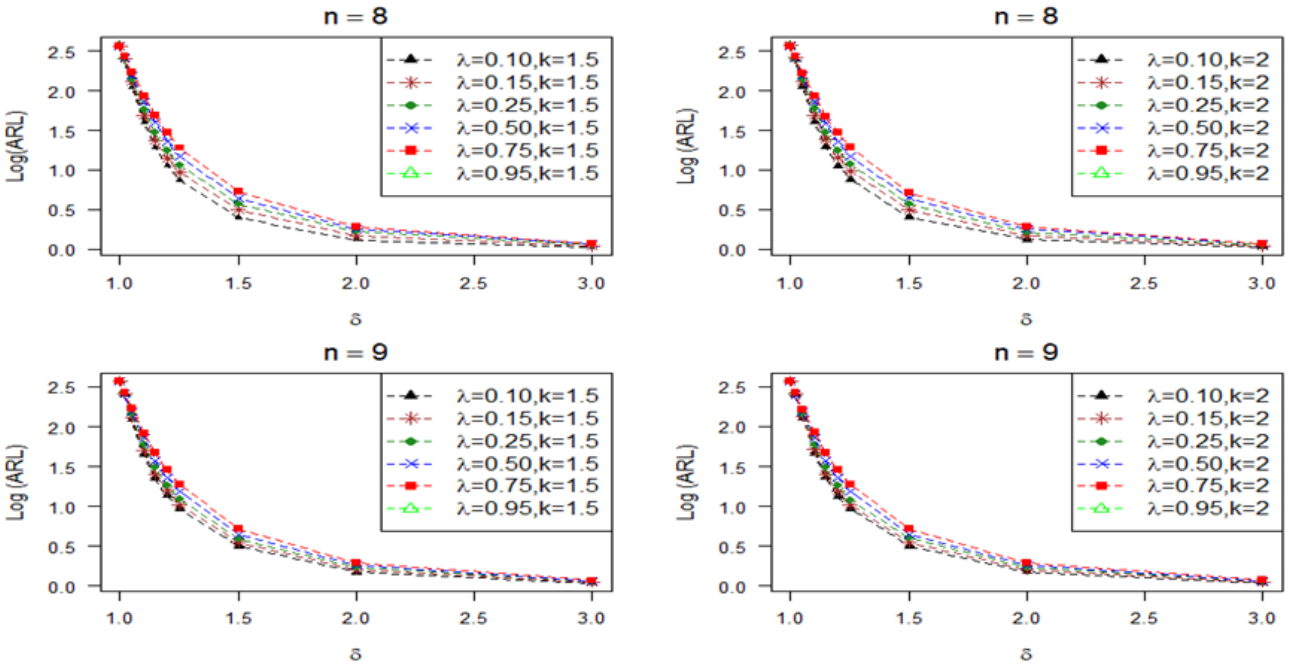

Figure 8: ARL_1 of the Proposed RAEWMA-RSS chart for the MAD when $n = 8, 9$, and $k = 1.5, 2$.

5. Manufacturing application

An application based on real-world data on the inside diameter of an engine's piston rings has been developed to showcase the idea. An engine's piston rings play an important role in the engine's operation. Piston rings play a critical role in sealing the combustion chamber and regulating gas pressure, thereby enhancing heat transfer from the piston to the cylinder wall. Additionally, they maintain the engine's oil level between the cylinder walls and the pistons. Every piston has at least two piston rings, each with a different function. The piston ring's size is critical since it is installed on the piston's outer surface. Normally, the standard piston ring size for an engine is 74 mm ±0.05 (cf. Figure 9). The complete diagram of piston rings and the inner view of the automobile engine are displayed in Figure 10. For the demonstration of the proposal, the measurement of the inside diameter size of an engine's piston ring is considered the interesting variable of the study, and this data set has been taken from a book (cf. [26]). The piston-

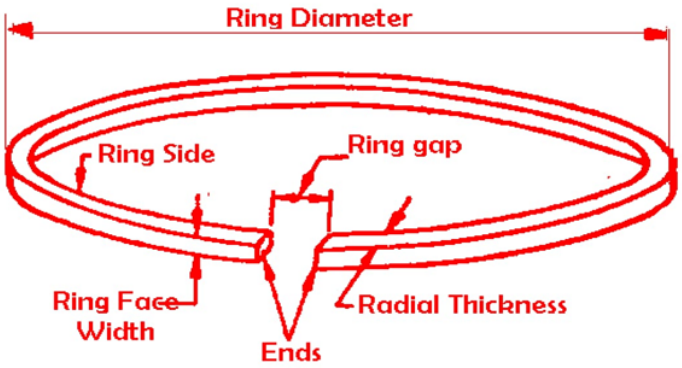

Figure 9: The diameter of the piston-ring.

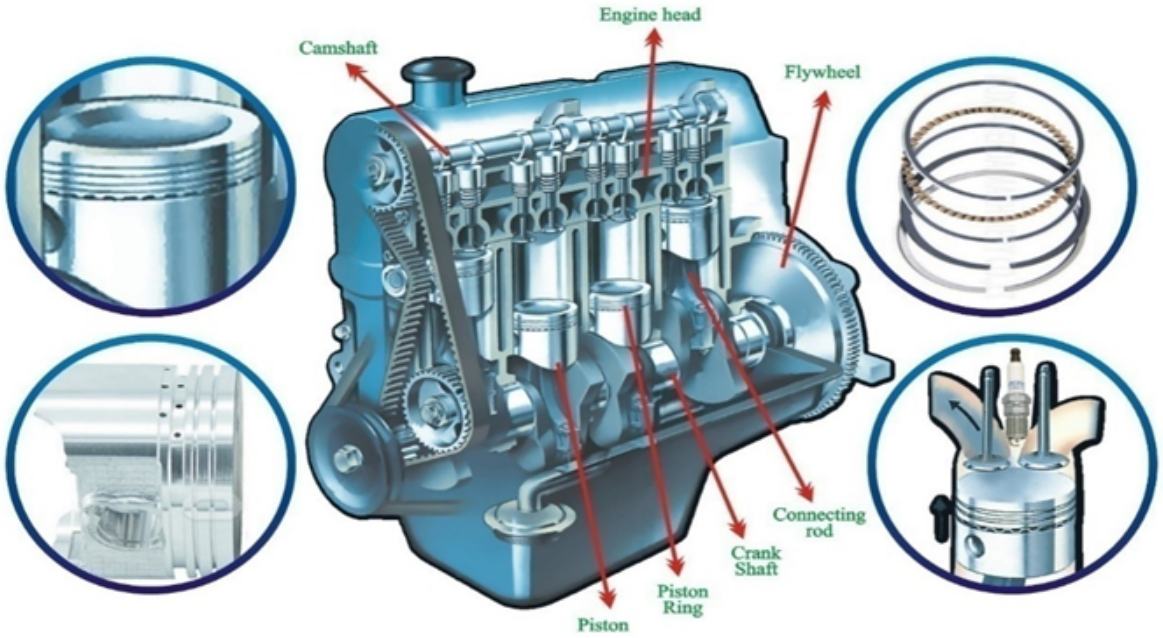

Figure 10: The inner view of the automobile engine.

ring inside-diameter measurements, with process target information centered around an in-control mean of 74.0032 and standard deviation 0.01038, and the control limits are calibrated to achieve ARL_0 of 370. The proposed AEWMA-RSS charts for different dispersion estimators display 40 plotting subgroups: the first 25 constitute Phase I (in-control period), and the remaining 15 constitute Phase II (monitoring period). The 40 subgroups of size 5 are obtained under ranked set sampling (RSS). Specifically, for each sampling cycle, $n = 5$ candidate observations will first be drawn from the available piston-ring measurements. These five observations will be ranked from smallest to largest using their measured inner diameters. From the first set, the smallest-ranked unit will be retained; from the second set, the second-ranked unit will be retained; this process will continue until, from the fifth set, the largest-ranked unit is retained. The five retained observations will then form one RSS subgroup of size 5. Repeating this process generates the 25 Phase I RSS subgroups, and the additional 15 Phase II RSS subgroups used for monitoring. For each subgroup, the dispersion statistics of interest (e.g., SD, Range, MAD, and IQR) are computed, and the resulting statistics are then plotted on the corresponding RAEWMA-RSS chart.

Figures 11-14 display the charting statistics for proposed AEWMA-RSS charts based on different dispersion estimators under RSS, showing that all Phase I points for all charts remain within the control limits, indicating an in-control reference period. Figure 11, based on the Range estimator, does not produce an out-of-control signal in the monitoring period. Figures 12 and 13, based on the MAD and IQR estimators, show that, in Phase II, five points exceed the upper control limit, signaling an out-of-control increase in dispersion. Figure 14, based on the SD estimator, shows 6 points that fall outside the control limits, indicating that these robust estimators can detect the increase in variability that the Range chart fails to identify. From this viewpoint, the real-data results are meaningful: the SD, MAD, and IQR-based RAEWMA-RSS charts can identify emerging variability during the monitoring phase, whereas the Range-based chart is comparatively less responsive.

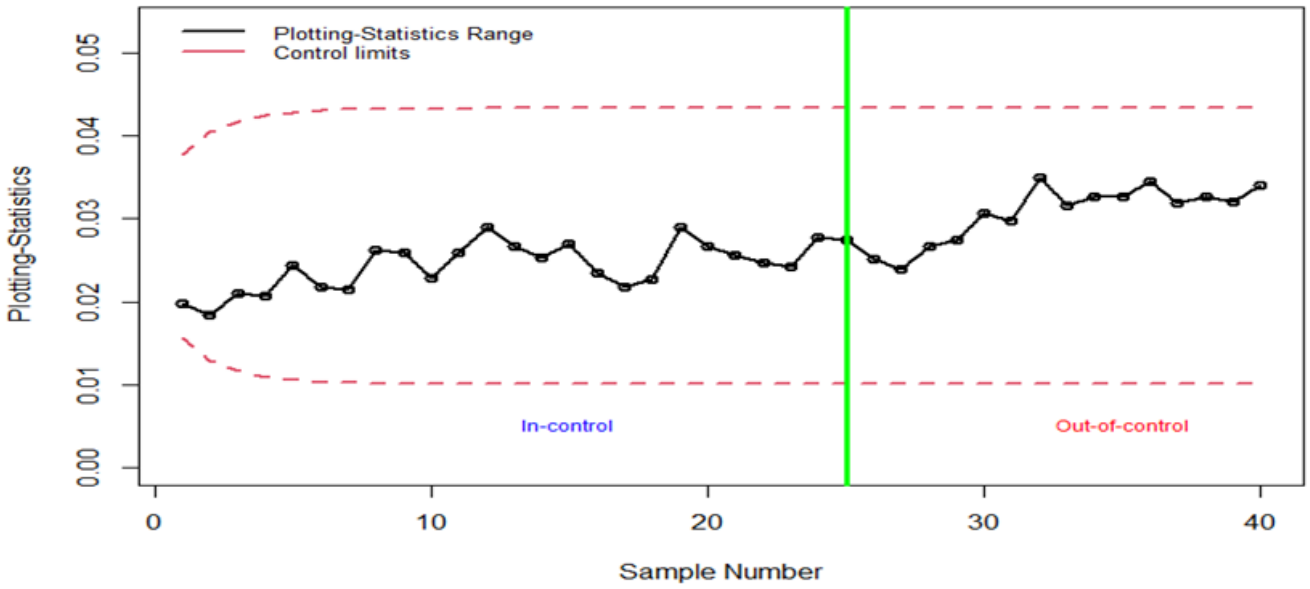

Figure 11: A range-based control chart based on piston-ring measurement.

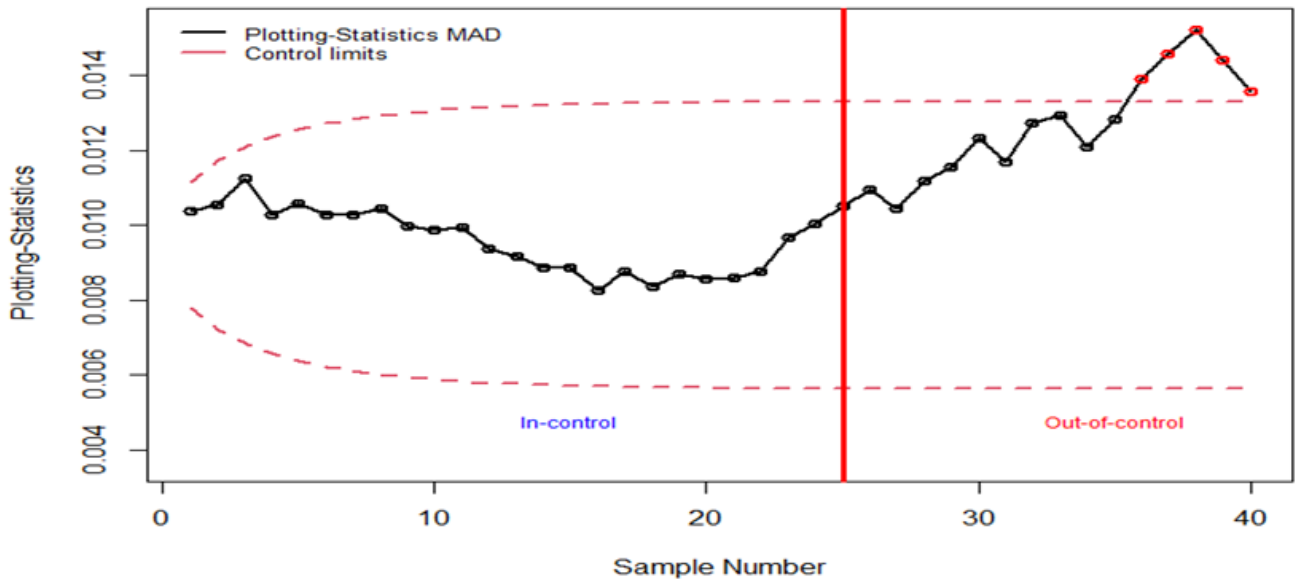

Figure 12: A MAD-based control chart based on piston-ring measurement.

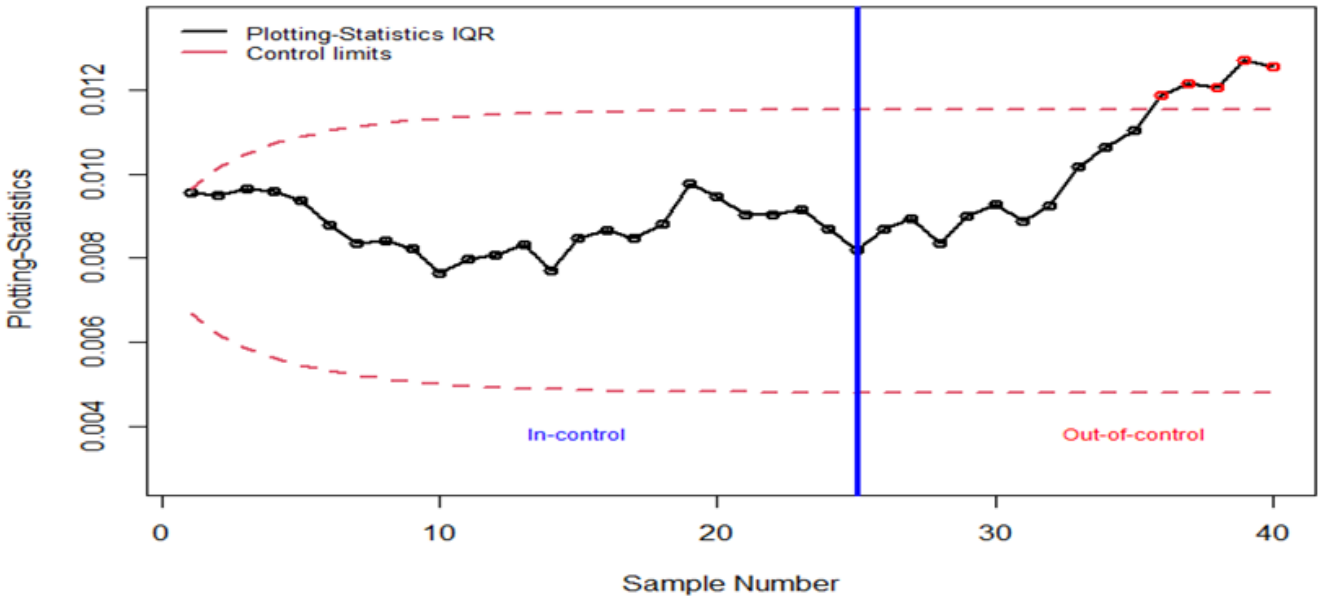

Figure 13: A IQR-based control chart based on piston-ring measurement.

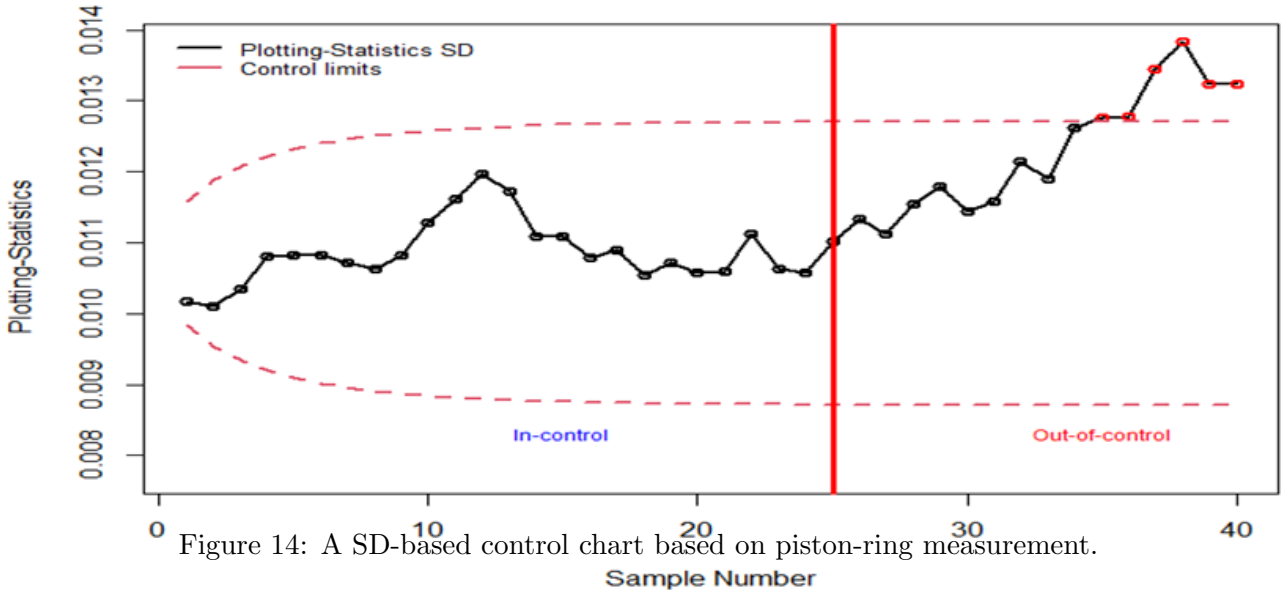

Figure 14: A SD-based control chart based on piston-ring measurement.

6. Summary and Conclusion

This study proposed a Robust Adaptive EWMA (RAEWMA-RSS) control chart for monitoring process dispersion under a ranked set sampling (RSS) framework. By integrating adaptive EWMA structures with robust dispersion estimators such as Range, Standard Deviation (SD), Interquartile Range (IQR), and Median Absolute Deviation (MAD). The simulation study, based on extensive Monte Carlo experiments and a target ARL_0 of 370, demonstrated that the proposed charts maintain consistent in-control performance while significantly improving out-of-control detection. Among the estimators, the SD-based RAEWMA-RSS chart exhibited the best overall performance, particularly for detecting small-to-moderate shifts in dispersion at higher values of the smoothing constant, followed by the IQR-based chart. The MAD estimator provided strong robustness but with relatively slower detection, while the Range-based chart showed the weakest performance. The real-data application using piston-ring manufacturing data further validated the practical effectiveness of the proposed method. The results showed that the robust adaptive charts (IQR, SD, and MAD) detected increases in process variability during the monitoring phase, whereas the Range-based chart failed to signal such changes. These findings highlight the advantage of combining robust estimation with adaptive smoothing and RSS, particularly in industrial environments where data may deviate from ideal assumptions. Overall, the proposed RAEWMA-RSS framework provides a flexible, robust, and efficient tool for dispersion monitoring, with clear advantages over conventional methods.

Acknowledgement

The first author was supported by the Office of Research and Graduate Studies at the University of Sharjah, United Arab Emirates (Competitive Grant Project No. 25021440172).

References

[1] T. Abbas, T. Mahmood, M. Riaz, and M. Abid. Improved linear profiling methods under classical and bayesian setups: An application to chemical gas sensors. *Chemometrics and Intelligent Laboratory Systems*, 196:103908, 2020. 4

[2] T. Abbas, F. Rafique, T. Mahmood, and M. Riaz. Efficient phase ii monitoring methods for linear profiles under the random effect model. *IEEE Access*, 7:148278–148296, 2019. 1

[3] T. Abbas, M. Riaz, B. Javed, and M. Abujiya. A new scheme of dispersion charts based on neoteric ranked set sampling. *Aims Math*, 8(8):17996–18020, 2023. 1

[4] T. Abbas, B. Zaman, A. Atir, M. Riaz, and S. Akbar Abbasi. On improved dispersion control charts under ranked set schemes for normal and non-normal processes. *Quality and Reliability Engineering International*, 35(5):1313–1341, 2019. 1

[5] Z. Abbas, T. Abbas, H. Z. Nazir, and M. Riaz. A novel adaptive cusum system for efficient process mean monitoring: An application in piston ring manufacturing process. *Alexandria Engineering Journal*, 106:87–100, 2024. 4

[6] S. A. Abbasi. Location charts based on ranked set sampling for normal and non-normal processes. *Quality and Reliability Engineering International*, 35(6):1603–1620, 2019. 1

[7] S. A. Abbasi, T. Abbas, and N. A. Adegoke. Efficient cv control charts based on ranked set sampling. *IEEE Access*, 7:78050–78062, 2019. 4

[8] M. Abid, M. Sun, A. Shabbir, M. Bakr, and T. Abbas. An enhanced nonparametric quality control chart with application related to industrial process. *Scientific Reports*, 14(1):13561, 2024. 4

[9] A. Abou El-Ela, H. A. Mosalam, and R. A. Amer. Optimal control design and management of complete dc-renewable energy microgrid system. *Ain Shams Engineering Journal*, 14(5):101964, 2023. 1

[10] S. Akram, T. Afzal, A. Ali, et al. Construction of optimal derivative free iterative methods for nonlinear equations using lagrange interpolation. *Journal of Prime Research in Mathematics*, 16(1):30–45, 2020. 2.1

[11] A. Ali, T. Mahmood, H. Z. Nazir, I. Sana, N. Akhtar, S. Qamar, and M. Iqbal. Control charts for process dispersion parameter under contaminated normal environments. *Quality and Reliability Engineering International*, 32(7):2481–2490, 2016. 1

[12] M. Aslam, K. Khan, M. Albassam, and L. Ahmad. Moving average control chart under neutrosophic statistics, aims math. 8 (2023), 7083–7096. 4

[13] H. Baskoroputro, F. Bhatti, H. M. Humza, and A. Y. Zakiyyah. The implementation of hosoya index and hosoya polynomial into some graphs related to cycles. *Journal of Prime Research in Mathematics*, 20(1):15–22, 2024. 2.1

[14] T. M. Beasley, S. Erickson, and D. B. Allison. Rank-based inverse normal transformations are increasingly used, but are they merited? *Behavior genetics*, 39(5):580–595, 2009. 1

[15] G. Capizzi and G. Masarotto. An adaptive exponentially weighted moving average control chart. *Technometrics*, 45(3):199–207, 2003. 1, 2.1, 2.1

[16] Z. Chen. On ranked-set sample quantiles and their applications. *Journal of Statistical Planning and Inference*, 83(1):125–135, 2000. 1

[17] A. H. Elmetwaly, A. A. ElDesouky, A. I. Omar, and M. A. Saad. Operation control, energy management, and power quality enhancement for a cluster of isolated microgrids. *Ain Shams Engineering Journal*, 13(5):101737, 2022. 1

[18] A. Haq. A new adaptive ewma control chart using auxiliary information for monitoring the process mean. *Communications in Statistics-Theory and Methods*, 47(19):4840–4858, 2018. 1

[19] T. P. Hettmansperger. The ranked-set sample sign test. *Journal of Nonparametric Statistics*, 4(3):263–270, 1995. 3.1

[20] S. Hussain, T. Mahmood, M. Riaz, and H. Z. Nazir. A new approach to design median control charts for location monitoring. *Communications in Statistics-Simulation and Computation*, 51(7):3553–3577, 2022. 4

[21] A. Javed, T. Abbas, N. Abbas, and M. Riaz. Designing bayesian paradigm-based cusum scheme for monitoring shape parameter of the inverse gaussian distribution. *Computers & Industrial Engineering*, 192:110235, 2024. 4

[22] W. Jiang, L. Shu, and D. W. Apley. Adaptive cusum procedures with ewma-based shift estimators. *Iie Transactions*, 40(10):992–1003, 2008. 1

[23] I. Khan, T. Abbas, and F. R. Albogamy. Optimizing lognormal process monitoring with bayesian approach for industrial engineering applications. *Quality and Reliability Engineering International*, 41(4):1483–1494, 2025. 4

[24] J. Law. Robust statistics—the approach based on influence functions, 1986. 2.2.4

[25] B. MacCarthy and T. Wasusri. A review of non-standard applications of statistical process control (spc) charts. *International Journal of Quality & Reliability Management*, 19(3):295–320, 2002. 1

[26] D. C. Montgomery. *Introduction to statistical quality control*. John wiley & sons, 2020. 5

[27] H. Z. Nazir, T. Hussain, N. Akhtar, M. Abid, and M. Riaz. Robust adaptive exponentially weighted moving average control charts with applications of manufacturing processes. *The International Journal of Advanced Manufacturing Technology*, 105(1):733–748, 2019. 1

[28] H. Z. Nazir, M. Riaz, R. J. Does, and N. Abbas. Robust cusum control charting. *Quality Engineering*, 25(3):211–224, 2013. 1

[29] E. S. Page. Continuous inspection schemes. *Biometrika*, 41(1/2):100–115, 1954. 1

[30] Z. Rasheed, M. Khan, S. M. Anwar, M. U. Aslam, S. A. Lone, and S. A. Almutlak. Designing an efficient adaptive ewma model for normal process with engineering applications. *Ain Shams Engineering Journal*, 15(9):102904, 2024. 4

[31] Z. Raza. Leap zagreb connection numbers for some networks models. *Indonesian Journal of Chemistry*, 20(6):1407–1413, 2020. 1, 2.1

[32] Z. Raza and A. Ali. Bounds on the zagreb indices for molecular (n, m)-graphs. *International Journal of Quantum Chemistry*, 120(18):e26333, 2020. 2.1

[33] M. Riaz, T. Mahmood, S. A. Abbasi, N. Abbas, and S. Ahmad. Linear profile monitoring using ewma structure under ranked set schemes. *The International Journal of Advanced Manufacturing Technology*, 91(5):2751–2775, 2017. 1

[34] S. W. Roberts. Control chart tests based on geometric moving averages. *Technometrics*, 42(1):97–101, 2000. 1

[35] A. Shafqat, Z. Huang, and M. Aslam. Design of x-bar control chart based on inverse rayleigh distribution under repetitive group sampling. *Ain Shams Engineering Journal*, 12(1):943–953, 2021. 4

[36] W. A. Shewhart. Quality control charts. *The Bell System Technical Journal*, 5(4):593–603, 1926. 1

[37] F. Touqeer, T. Mahmood, M. Riaz, and N. Abbas. On developing linear profile methodologies: a ranked set approach with engineering application. *Journal of Engineering Research*, 8(2):203–225, 2020. 1

[38] E. Yashchin. Some aspects of the theory of statistical control schemes. *IBM Journal of Research and Development*, 31(2):199–205, 1987. 1